J Mater Sci (2011) 46:7923–7930
DOI 10.1007/s10853-011-5925-6

LETTER

Effects of supercooling and organic solvent on the formation of a silk sponge with porous 3-D structure, and its dynamical and structural characterization using solid-state NMR

Tsunenori Kameda · Tomoko Hashimoto · Yasushi Tamada

Published online: 16 September 2011

Introduction

A widely accepted feature of the silk generated by silkworms is its impressive mechanical properties. Aside from its direct use as silk fibers, silk protein can also be dissolved and converted into hydrogels [1], films [2], fibers [3], beads [4], electrospun nonwoven fibroin [5], and sponges, leading to great versatility in use. Silk sponge is the generic name for the porous 3-D structure made of silk fibroin. Many methods have been explored for the formation of a silk sponge. Freeze-drying of fibroin hydrogels [1] or fibroin solution in the presence of an appropriate cross-linker [6] yields silk sponges. Salt leaching and gas foaming are also used to form silk sponges [7, 8]. Silk sponges can also formed by repeated freezing and thawing [9].

One of the authors developed an original method to prepare silk sponges, which is shown in Fig. 1 [10]. The process involved freezing and thawing an aqueous solution of fibroin in the presence of a small amount of an organic solvent. The advantage of this method is that it does not require freeze-drying, chemical cross-linking, or polymeric materials. The influences of various concentrations of organic solvents and fibroin on sponge structure were investigated [10]. The compressive modulus and tensile strength were changed depending on the concentration used.

The fibroin sponge prepared by our process can be used as a tissue-engineering scaffold because it is formed from biocompatible, pure silk fibroin and has both a porous structure and mechanical properties that are suitable for cell growth and handling [10–13]. For 3 weeks, MC3T3 cells proliferated in the sterilized fibroin sponge. In order to develop a technique to control the fibroin sponge's porous structure and improve its quality (uniformity, reproducibility, etc.) so that it can be used as a scaffold, the process for fibroin sponge formation must be clarified.

Determination of the secondary structure of a silk sponge was previously attempted using X-ray diffraction (XRD) and Fourier transform infrared (FTIR) spectroscopy [10], both of which indicated the coexistence of Silk I and II crystalline structures in the dried sponge. Since there are structural differences between dried fibroin sponges and the freeze-dried fibroin formed from an aqueous solution without any sponge formation, we concluded that the secondary structure of fibroin is transformed from non-crystalline random coils into Silk I and II crystalline structures during the sponge formation process. However, the process by which a non-crystalline structure transforms into a crystalline structure needs to be explored in greater detail because it is possible that this transformation occurs not during sponge formation but during the drying process when the samples are dried for XRD and FTIR experiments. Therefore, direct observation of the structural changes that occur during sponge formation during wetting must be investigated. Moreover, only a dried silk sponge was examined in previous XRD and FTIR experiments; hence, no information regarding the molecular structure and dynamics of a wet sponge are available. Site-specific information, such as the conformation of each individual amino acid, is also difficult to determine from XRD and FTIR experiments.

Solid-state NMR is an excellent tool for determining both the molecular structure and dynamics in both the crystalline and non-crystalline domains in silk materials

T. Kameda · T. Hashimoto · Y. Tamada (✉)
National Institute of Agrobiological Sciences,
Tsukuba 305-8634, Japan
e-mail: ytamada@affrc.go.jp

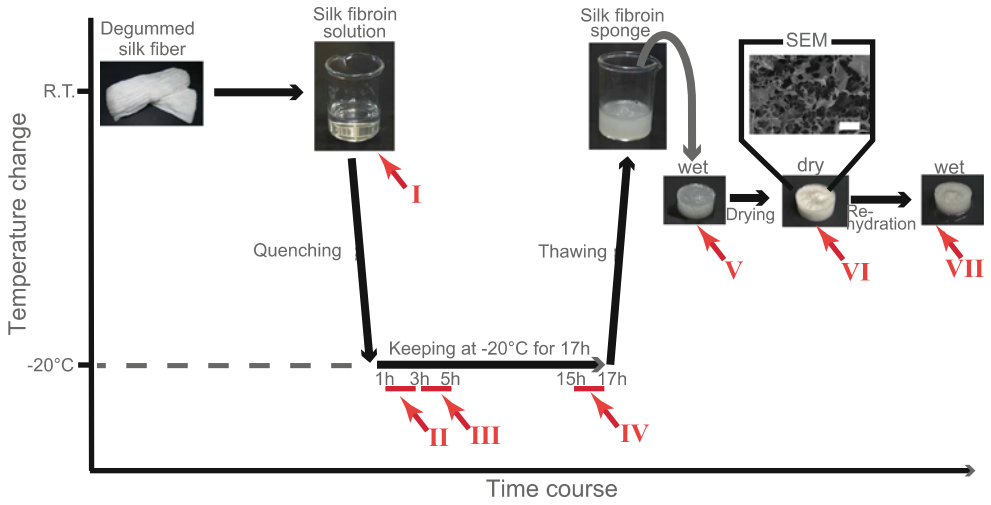

Fig. 1 Schematic drawing of a process for the preparation of a silk fibroin sponge. The silk sponge is obtained by wetting. Photographs of the silk sponge after drying and rehydration are also shown. Scanning electron micrograph (SEM) indicates the porous structure of the silk fibroin sponge in the dried state. SEM observation was performed using JSM-6301F (JEOL Ltd, Japan), and scale bar in the SEM image indicates 100 μm. The numbers I–VII correspond to the stages in the process of sponge formation and the silk fibroin in each stage observed with NMR (see text)

[14, 15]. A ^{13}C solid-state NMR experiment under MAS was previously used to obtain site-specific information such as the conformation and dynamics of each individual amino acid because each amino acid can be identified by its distinct ^{13}C peaks. Furthermore, solid-state NMR allowed us to observe the spectra of the samples nondestructively, regardless of the degree of hydration of the sample under any temperature condition. One of the authors studied process of fiber formation from fibroin in liquid silk, using solid-state NMR [16]. That study revealed that the silk fibroin of *Samia cynthia ricini* initially had a mobile α-helix structure in liquid silk, and then, the gradual and monotonic slowdown of the overall molecular motions led to molecular aggregation, leading to the formation of a rigid β-sheet structure during transformation from the liquid state to the solid state. Therefore, it was assumed that the sponge formation process can be observed using solid-state NMR.

The objectives of this study are as follows: (1) clarification of the molecular structure and dynamics of the fibroin sponge in a hydrated state; (2) understanding the structural changes in fibroin molecules in DMSO-containing aqueous solution under the cooling condition.

Materials and methods

Materials

The process for preparing a silk fibroin sponge is shown in Fig. 1. Fibroin aqueous solutions were obtained by dissolving degummed silk fibroin from *Bombyx mori* with 9.0 M lithium bromide solution, followed by dialysis against water. Dimethyl sulfoxide (DMSO) was added gradually, with stirring, to a fibroin aqueous solution at the determined volume depending on the final concentration of the fibroin (2 wt%) and DMSO (1 vol%). The mixed solution was poured into a mold. The solution was quenched at −20 °C and kept at this temperature for 17 h. Then, the mold was thawed at room temperature to yield a porous fibroin 3-D structure. The fibroin sponges were washed by immersion in water or buffer solution to remove the solvents.

While preparing the silk sponge (Fig. 1), NMR measurements were carried out for the silk fibroin at seven different stages, indicated by I–VII in Fig. 1. Stage I is the silk fibroin solution at room temperature. Stage II is the silk fibroin solution at 1–3 h after quenching at −20 °C, and stage III is the silk fibroin solution at 3–5 h, and stage IV is the silk fibroin solution at 15–17 h. Stage V is the state of the silk sponge after washing to remove the DMSO solvent. Stage VI is the dry sample, which is obtained after drying the silk sponge in Stage V. Stage VII is the rehydration state, which is after the dried sponge in Stage VI is wet.

Methods

^{13}C Solid-state nuclear magnetic resonance (NMR)

High-resolution solid-state ^{13}C NMR spectra were obtained using an Infinity 300 spectrometer (Agilent/Chemagnetics, Fort Collins, CO, USA) operating at a ^{13}C NMR frequency of 75.4 MHz. The samples were spun at the magic angle at 2.5–4.0 kHz in a solid-state probe in a 7.5-mm ϕ zirconia

rotor. For normal ^{13}C 90° single-pulse (direct polarization; DP) experiments, we used a ^{13}C NMR 90° pulse length of 5.0 μs with high-power ^{1}H decoupling by the continuous wave (CW) method. For the cross-polarization (CP) experiments, we used a ^{1}H NMR 90° pulse length of 5.0 μs and ^{1}H-^{13}C CP contact of 50 kHz. The power of ^{1}H decoupling was 80 kHz. For all experiments, the repetition time for all CP experiments was 3.0 s. All spectra were calibrated using adamantane as the standard because the CH_2 peak at 29.5 ppm gives shift values referenced to TMS carbon at 0 ppm.

A solid-state probe in a 7.5-mm ϕ zirconia rotor (Chemagnetics) was used. For the wet samples, the cap of the rotor was sealed using epoxy resin to prevent fluid leakage. The samples were spun at the magic angle at 5.0 kHz. For the CP-magic angle spinning (MAS) experiments, a ^{1}H NMR 90° pulse length of 5.0 μs and ^{1}H-^{13}C CP contact of 50 kHz were employed. The power of ^{1}H decoupling was 60 kHz.

Low temperature experiments corresponding to stages II–IV (Fig. 1) were carried out as follows. An aqueous solution of silk (2 wt%) was enclosed in an NMR MAS tube, and epoxy resin was used to fill in the gap between the cap and tube. The sample tube was then quenched at −20 °C under spinning at 2.5 kHz.

For the normal ^{13}C 90° single-pulse (DP) experiments, we used a ^{13}C NMR 90° pulse length of 2.5 μs with high-power ^{1}H decoupling with the Two Pulse Phase Modulation (TPPM) method.

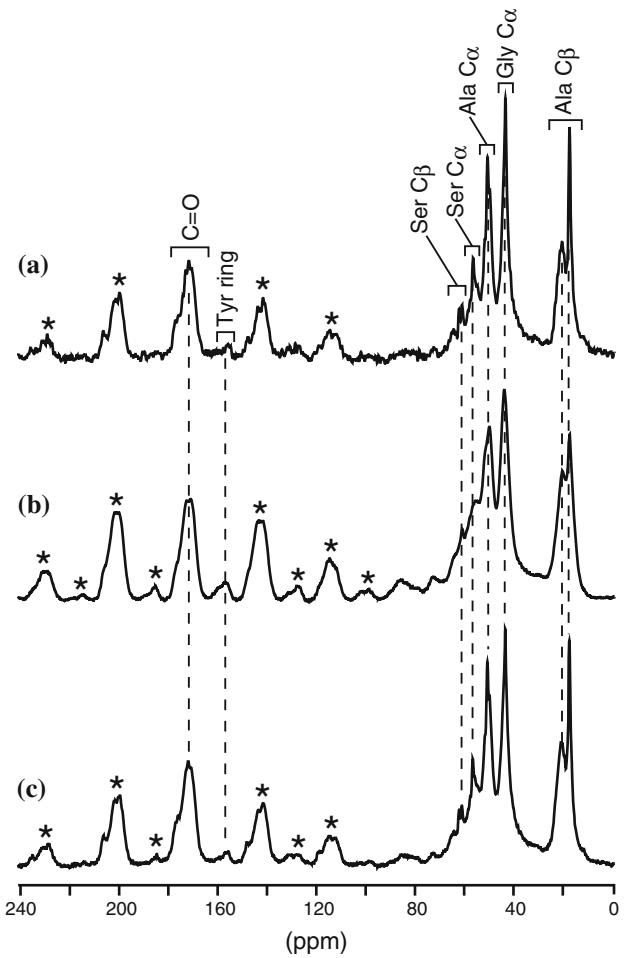

Fig. 2 The ^{13}C CP/MAS NMR spectrum of the as-prepared (hydrated state) (**a**), dried (**b**), and rehydrated (**c**) fibroin sponges. The samples were spun at 2.5 kHz. Spinning sidebands in the spectra are denoted with *asterisks*

Results and discussion

Molecular structure of the hydrated silk sponge

The prepared fibroin sponge was rinsed with water for 12 h to remove the remaining DMSO. Then, the rinsed sample, which corresponds to stage V in Fig. 1, was loaded into an NMR sample tube while maintaining the hydration. The ^{13}C CP/MAS spectrum of the hydrated sponge is shown in Fig. 2a.

As described below, the residual DMSO solvent in the sponge resulted in a sharp peak at 39.5 ppm. The fact that no peak was observed at around 40 ppm (Fig. 2a) indicates that the DMSO is completely removed by the rinsing process.

Expansion of the C_α/C_β spectral regions in Fig. 2a is shown in Fig. 3a, together with the expansion spectra for the degummed *B. mori* cocoon (Fig. 3d) and the freeze-dried fibroin in its aqueous solution (Fig. 3e) for comparison. Peak assignments in Fig. 3a were made on the basis of data from previous references [17]. It was established that the ^{13}C chemical shifts of the C_α, C_β, and C=O carbons depended on the conformation of the protein backbone. The chemical shift dependence allowed the use of ^{13}C CP/MAS NMR to determine the conformation of the silk fibroin. The typical spectra of Silk II (β-sheet)-rich and random coil-rich silk fibroin are shown in Fig. 3d and e, respectively.

The Ala residue exhibited an especially large change in the chemical shift with the secondary structure [14]. The peaks at 17.2 and 50.7 ppm in Fig. 3a were within the experimental error of the chemical shifts of Ala residues with a random coil structure. The ratios of the intensities of these random coils to those of Silk II (β-sheet) peaks were found to be larger in Fig. 3a than in Fig. 3d and e. This result indicates that the Ala residue in the silk sponge had a random coil-rich structure. Peaks also appeared at 20.5 and 49.6 ppm, indicating that a Silk II crystal system with a β-sheet conformation existed in the silk sponge. Moreover, the shoulder peaks on the right side of the peak at 17.2 ppm and left side of the peak at 50.7 ppm (both peaks are

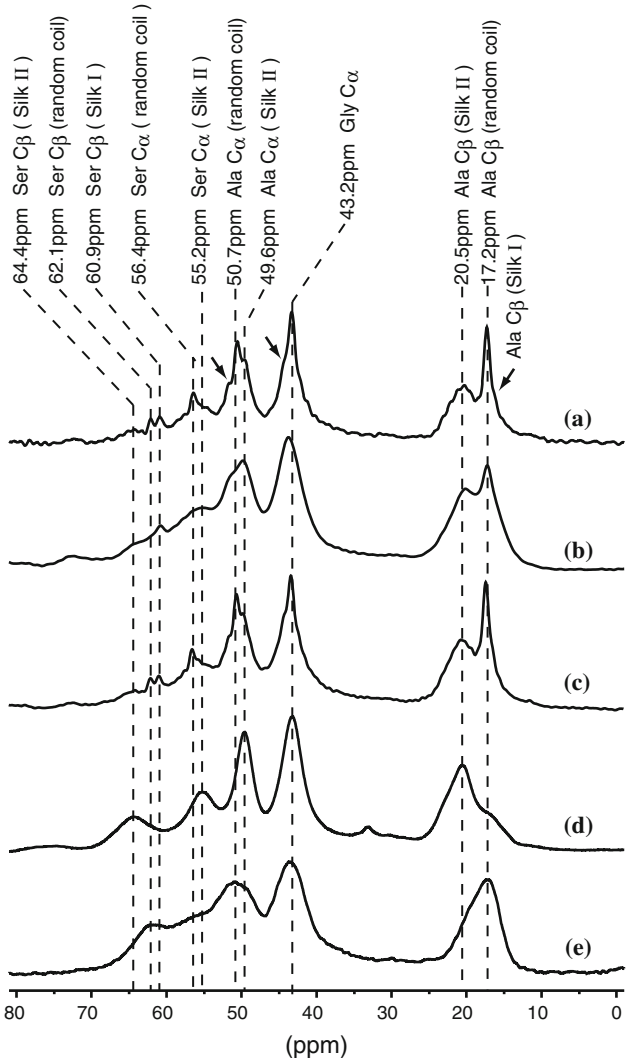

Fig. 3 Enlargement of the amino acid C_α/C_β peak region of the ^{13}C CP/MAS NMR spectra for the as-prepared (hydrated state) (**a**), dried (**b**), and rehydrated (**c**) fibroin sponges, together with those for the degummed *B. mori* cocoon silk fiber in the dry state (**d**) and the freeze-dried fibroin of its aqueous solution (**e**) for comparison

indicated by arrows in Fig. 3a) were attributed to the Silk I crystal system. The chemical shift value of the C_β peak in the Silk I crystal is reported to be 16.5 ppm [17]. The fact that a Silk I crystal system existed in the silk sponge is supported by the results of our previous XRD experiment. These results confirm that the silk sponge predominately has a random coil structure with some amount of crystalline domains with Silk I and II crystal systems in the hydrated state.

With regard to the Ser residue in the hydrated sponge, peaks attributable to Ser C_β in a random coil and Silk II (β-sheet) system were observed at 62.1 and 64.4 ppm, respectively, as shown in Fig. 3a. Moreover, an additional Ser C_β peak was observed at 60.9 ppm, which was attributed to the carbon in the Silk I crystal [17]. Therefore, the ^{13}C NMR peak for the Ser residue served as proof of the existence of the Silk I crystal in the silk sponge, although no distinct peak attributable to the Ser C_α in the Silk I crystal, which is known to resonate at 58.0 ppm, was observed. The two Ser C_α peaks at 55.2 and 56.4 ppm were attributed to the carbons in the Silk II crystal and random coil, respectively.

The chemical shift of the Gly C_α is rather ambiguous for the most commonly observed conformations; hence, little information could be obtained from the isotropic chemical shift [14]. However, an asymmetrical peak of Gly C_α was observed at around 43 ppm in Fig. 3a, indicating the coexistence of Gly residues in the multi-structures. A previous study reported that the peaks attributable to the Gly C_α in Silk I and II crystals are observed at 43.8 and 43.1 ppm, respectively [17]. Therefore, the main peak at 43.2 ppm was assigned to the Silk II crystal system. Moreover, this main peak at 43.2 ppm is considered to overlap with the peak attributable to the Gly C_α in the random coil because the peak of Gly C_α in the fibroin aqueous solution was observed at 43.2 ppm as described below. The peak attributable to the Gly C_α in Silk I was observed at the shoulder peak on the left side of the main peak at 43.2 ppm (corresponding peaks are indicated with arrows in Fig. 3a). This finding also supports the existence of a Silk I crystal in the silk sponge.

Molecular dynamics of a hydrated silk sponge

The sponge was dried and then rehydrated, which corresponds to the samples in the stages VI and VII, respectively. The ^{13}C CP/MAS spectra for the dried and rehydrated sponge are shown in Fig. 3b and c, respectively. Since the line shapes and chemical shift values for all carbon signals between Fig. 3a and c were mostly identical, it was assumed that the molecular structure and dynamics in the hydrated state are almost recovered by rehydration. On the other hand, the ^{13}C CP/MAS spectrum of the dried sponge (Fig. 3b) was different from the spectra of the hydrated sponge (Fig. 3a and c). Peak broadening occurred due to drying, which indicated restricted molecular motion.

In order to examine the difference between the wet and dry sponges in detail, enlargements of the C_α/C_β and carbonyl regions of Figs. 3a and b were superimposed and are shown in Fig. 4a. The spectra of the wet and dry samples are represented with red and black lines in this diagram, respectively. This figure showed that the peak narrowing induced by hydration mainly occurred at the peaks attributed to the random coil, whereas almost no change was observed at the peaks attributed to the β-sheet (Silk II) crystalline structure. Peak narrowing occurs because of an increase in molecular motion. Therefore, the abovementioned result

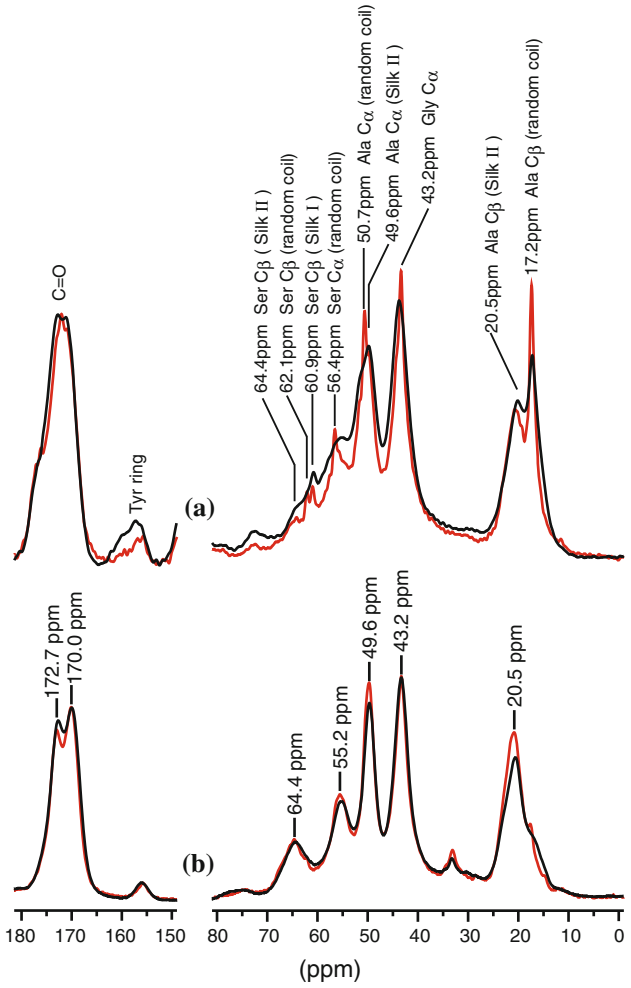

Fig. 4 Enlargement of the ^{13}C CP/MAS NMR spectra of the fibroin sponge in dried (**a**, *black-line*) and hydrated (**a**, *red-line*), and degummed silk fiber after drying (**b**, *black-line*) and hydration (**b**, *red-line*), showing the C=O and C_α/C_β regions

indicates that the change in dynamics occurred only in the random coil. The stabilization of the crystalline region by hydration might play an important role in stabilizing the shape of the sponge and preventing its shrinkage.

The ^{13}C CP/MAS spectra of the fibroin fiber of the degummed *B. mori* cocoon in hydrated and dried states are shown in Fig. 4b for comparison. Here, the period of immersion of the fibroin fiber in distilled water was identical to that for the silk sponge. Mostly, no change was found in the peak width upon wetting of the fibroin fiber (Fig. 4b), and therefore, the fibroin fiber underwent no change in dynamics, which was a notable difference between the fiber and the sponge. Moreover, comparison between Fig. 4a and b revealed that the number of random coils in the sponge was greater than that in the fiber. These results confirmed that hydration resulted in an increase in molecular motion in the random coils, and the large random coil domain was considered to lend flexibility to the fibroin sponge.

Since a number of peaks arising from different amino acids overlapped in the carbonyl (C=O) region, little detailed information on the structure was obtained from Fig. 3a. However, when we paid attention to the spinning side band (SSB) peaks in Fig. 2 (marked with asterisks in the figure), we found that the SSB patterns of the dry sponge differed from those of the wet sponge. That is, the intensity ratios of the sideband-to-isotropic peak for the wetted sponge were smaller than those for the dried sponge. Further, these ratios decreased by more than 25% on average. This finding suggests that the mobility (fast on the NMR time scale of kHz) would lead to a partial averaging of the chemical shift tensor when the sponge was wetted [18].

Formation of the silk sponge

We considered that supercooling and temperature maintenance at −20 °C for a while played important roles in the formation of the fibroin sponge structure. In order to investigate the structural change from the solution to the sponge state under quenching, we carried out a time series measurement of the ^{13}C CP/MAS NMR spectra for the DMSO-containing aqueous solution of fibroin at −20 °C (stages II–IV in Fig. 1). The 2-h acquisition to obtain the spectra started 1, 3, and 15 h after quenching at −20 °C and is shown in Fig. 5a, b, and c, respectively. In each spectrum, the signal-to-noise ratio of the fibroin peaks was rather low, which could be attributed to the lower fibroin concentration (2.0 wt%) and short acquisition time of 2 h.

The signal-to-noise ratios of peaks in C=O and C_α/C_β regions increased with time (Fig. 5a–c). This increase in the signal-to-noise ratios of the ^{13}C CP/MAS spectrum was attributed to a decrease in chain dynamics because decrease in chain mobility strengthened ^{1}H–^{13}C dipolar coupling, facilitating the CP process. Therefore, the change in the spectra shown in Fig. 5a–c indicated a decrease in chain dynamics with time. This decrease in chain dynamics was considered to be a result of aggregation for sponge formation.

In order to focus on two resonance lines of Ala C_α and C_β in Fig. 5, the enlargement of the C_α/C_β region in Fig. 5 is shown in Fig. 6. Figure 6e shows the enlargement of the C_α/C_β region of the ^{13}C DP spectrum of the DMSO-containing fibroin aqueous solution (Stage I in Fig. 1) at room temperature. A sharp peak was observed for Ala C_α at 17.2 ppm in Fig. 6e, which could be attributed to the random coil structure in the liquid state. This random coil peak was mainly observed in Fig. 6a, and no distinct peaks attributable to the β-sheet corresponding to the Silk II form were observed in this spectrum. This result indicated that

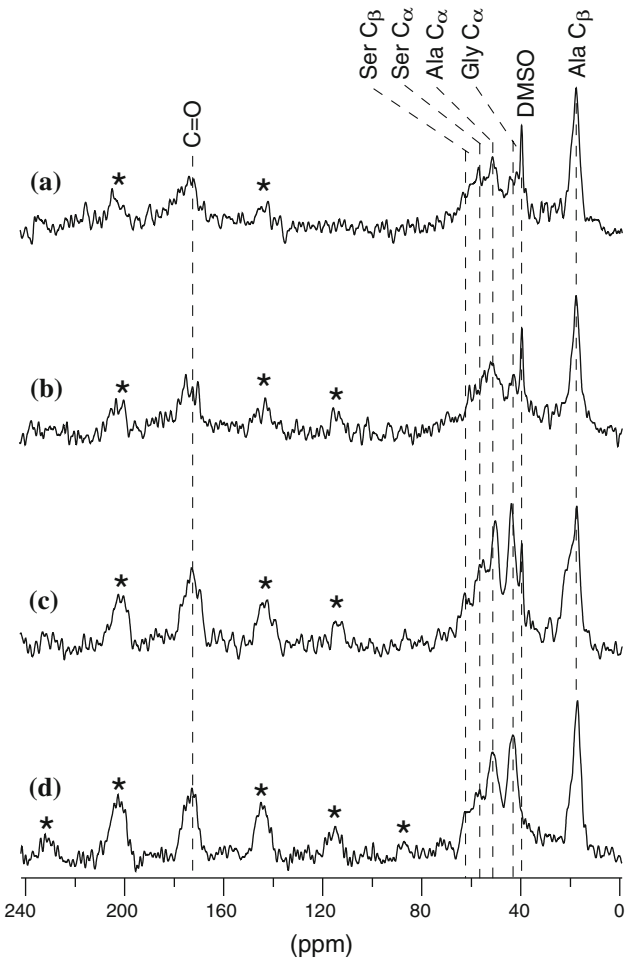

Fig. 5 The ^{13}C CP/MAS spectra of the DMSO-containing fibroin aqueous solution obtained with 2 h acquisition that started at 1 h (**a**), 3 h (**b**), and 15 h (**c**) after quenching at −20 °C, together with that of the DMSO-free fibroin aqueous solution after holding at −20 °C for 15 h (**d**)

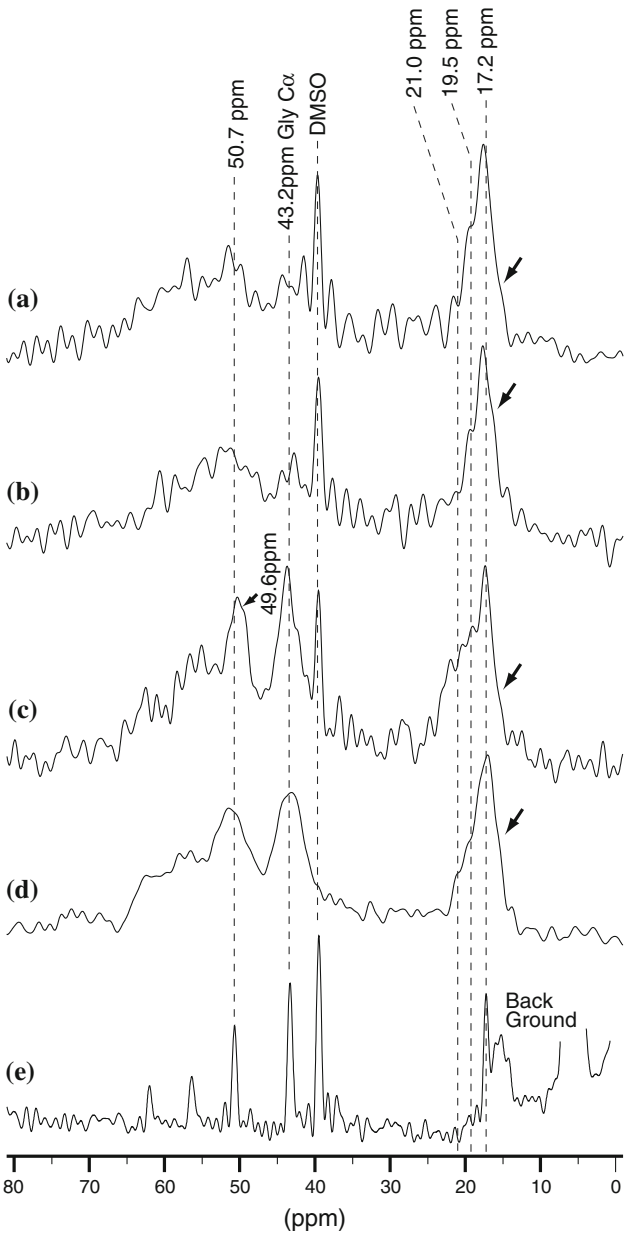

Fig. 6 Enlargement of the C_α/C_β region of the ^{13}C CP/MAS spectra of the DMSO-containing fibroin aqueous solution. Two hours acquisition started at 1 h (**a**), 3 h (**b**), and 15 h (**c**) after quenching at −20 °C, together with that of the DMSO-free fibroin aqueous solution after holding at −20 °C for 15 h (**d**) and the ^{13}C DP spectrum of the DMSO-containing fibroin aqueous solution at room temperature (**e**)

the random coil structure predominately exists at the beginning of quenching.

However, in Fig. 6a, note that a peak attributable to the Silk I crystal (indicated with an arrow in the figure) was observed, indicating that the crystalline structure with Silk I form was produced almost immediately after quenching at −20 °C.

In addition, a shoulder peak was clearly observed at around 19.5 ppm in Fig. 6a. This peak could be attributed to the fibroin component with restricted molecular motion because the peak at 19.5 ppm was absent in Fig. 6e. Moreover, this peak was different from the peak of Ala C_α attributed to the β-sheet structure, which was observed at 20.5 ppm as shown in Fig. 3b. Therefore, we concluded that the peak at 19.5 ppm could be attributed to the intermediate structure between the random coil and the β-sheet.

The line shape of Fig. 6b was almost identical to that of Fig. 6a, suggesting that no conformational change occurred within 5 h. However, the spectrum that accumulated within 15–17 h after quenching (Fig. 6c) changed markedly in Fig. 6a and b. In Fig. 6c, the shoulder peak at around 21 ppm and multiple C_α peaks at around 30–70 ppm were observed. The peak at 21 ppm could be attributed to the Ala C_β in the β-sheet structure. Moreover, the peak at 49.6 ppm that was attributed to the Ala C_β in the β-sheet (Fig. 3b) was observed as a shoulder peak in Fig. 6c. These results

suggest that a structural change in the β-sheet conformation occurred within 15 h after quenching at −20 °C.

In order to examine the influence of DMSO addition on sponge formation, the DMSO-free fibroin aqueous solution was quenched at −20 °C, and after leaving the quenched solution to stand for 15 h, the ^{13}C CP/MAS NMR spectrum was observed (Fig. 5d). Strong peaks were observed in Fig. 5d, which was similar to the spectrum of the DMSO-containing system (Fig. 5c). However, some critical differences were found in these spectra. In order to examine these differences in detail, an enlargement of the C_α/C_β region of Fig. 5d is shown in Fig. 6d and compared with Fig. 6c.

The peak width in Fig. 6d was broader than that in Fig. 6c. Moreover, the signal-to-noise ratio of Fig. 6d was larger than that of Fig. 6c, indicating stronger peak intensities in Fig. 6d. These results indicate that the fibroin generated from the DMSO-free aqueous solution (Fig. 6d) has lower molecular dynamics than that generated from the DMSO-containing solution (Fig. 6c). These findings suggest that aggregation of the fibroin generated from the DMSO-free aqueous solution was stronger than that generated from the DMSO-containing solution. This aggregation may promote sponge formation. However, in conflict with this consideration, no sponge formation occurred in the DMSO-free aqueous solution, and a silk sponge was produced only from the DMSO-containing aqueous solution. This result indicated that there is an important factor responsible for the sponge generation besides molecular aggregation. In Fig. 6c, the shoulder peaks attributable to the β-sheet were observed at 21.5 and 49.6 ppm. On the other hand, in Fig. 6d, although these shoulder peaks were observed at similar positions, the intensities of these peaks were smaller than those in Fig. 6c, indicating that a smaller amount of the β-sheet component was generated from the DMSO-free fibroin aqueous solution. Therefore, we considered that the existence of the DMSO solvent in the aqueous fibroin solution played a key role in the generation of the β-sheet, which proceeded rapidly when the solution was held at −20 °C. We conclude that β-sheet formation is essential for silk sponge formation.

Conclusion

In this study, we used ^{13}C solid-state NMR to investigate the following: (1) the molecular structure and dynamics of the fibroin sponge in a hydrated state, and (2) the mechanism by which a sponge structure is generated from the fibroin aqueous solution. The conclusions are as follows:

(1) The hydrated silk sponge comprised a random coil-rich structure, including some crystalline structures. In the crystal domain, Silk I and II crystal forms coexisted. The molecular motion in the random coil domain increased markedly when the sponge was hydrated. The larger existential amount of random coil and increasing amount of molecular motion in the random coil structure when the sponge was hydrated as compared to when the native silk fiber was considered are thought to be associated with the flexibility of the silk sponge during hydration. On the other hand, the crystal domain in the sponge was almost unchanged by hydration, which was considered to be associated with the high performance of the silk sponge during hydration.

(2) We found that supercooling during the freezing process and the freezing duration of the fibroin aqueous solution played an important role in determining the character of the fibroin sponge. The secondary structure of the fibroin in the aqueous solution presented a mainly random conformation at the start of freezing at −20 °C, and then, some amount of the random coil structure changed to the β-sheet conformation when held at −20 °C for 15 h. The formation of the β–sheet was promoted by the addition of DMSO in the fibroin aqueous solution. When the fibroin aqueous solution was free from DMSO, the degree of β-sheet content after freezing and thawing was quite low, and no sponge formation occurred. Organic solvents were indispensable for the formation of the fibroin sponge and important to fabricate a fibroin sponge with good mechanical strength.

Acknowledgements This study was supported in part by the Agri-Health Translational Research Project and Research and development project for application in promoting a new policy for Agriculture Forestry and Fisheries.

References

1. Kim UJ, Park JY, Li CM, Jin HJ, Valluzzi R, Kaplan DL (2004) Biomacromolecules 5(3):786
2. Lawrence BD, Omenetto F, Chui K, Kaplan DL (2008) J Mater Sci 43(21):6967. doi:10.1007/s10853-008-2961-y
3. Yao JM, Masuda H, Zhao CH, Asakura T (2002) Macromolecules 35(1):6
4. Hino T, Tanimoto M, Shimabayashi S (2003) J Colloid Interface Sci 266(1):68
5. Shao HL, Zhu JX, Hu XC (2007) Int J Biol Macromol 41(4):469
6. Li MZ, Ogiso M, Minoura N (2003) Biomaterials 24(2):357
7. Nazarov R, Jin HJ, Kaplan DL (2004) Biomacromolecules 5(3):718
8. Marcotte I, Byette F, Bouchard F, Pellerin C, Paquin J, Mateescu MA (2011) Polym Bull 67(1):159
9. Li MZ, Zhang CS, Lu SZ, Wu ZY, Yan HJ (2002) Polym Adv Technol 13(8):605

10. Tamada Y (2005) Biomacromolecules 6(6):3100
11. Aoki H, Tomita N, Morita Y, Hattori K, Harada Y, Sonobe M, Wakitani S, Tamada Y (2003) Biomed Mater Eng 13(4):309
12. Tomita N, Kambe Y, Takeda Y, Yamamoto K, Kojima K, Tamada Y (2010) Biomed Mater Eng 20(6):309
13. Kawakami M, Tomita N, Shimada Y, Yamamoto K, Tamada Y, Kachi N, Suguro T (2011) Biomed Mater Eng 21:53
14. Saito H, Tuzi S, Naito A (1998) Polysaccharides and biological system. Elsevier, Tokyo
15. Kameda T, Asakura T (2002) Dynamics of silk fibroin studied with NMR spectroscopy. Academic Press, London
16. Nakazawa Y, Nakai T, Kameda T, Asakura T (1999) Chem Phys Lett 311(5):362
17. Asakura T, Demura M, Date T, Miyashita N, Ogawa K, Williamson MP (1997) Biopolymers 41(2):193
18. van Beek JD, Kummerlen J, Vollrath F, Meier BH (1999) Int J Biol Macromol 24(2–3):173